Seismic performance of RC columns retrofitted with CFRP Strips

H. Araki & R. Sato
Hiroshima University, Japan

K. Kabayama
Shibaura Institute of Technology, Japan

M. Nakata
Kosei Kensetsu Corporation, Japan

ABSTRACT: Reinforced concrete columns of the rail-way structures were severely damaged at 1995 Hyogoken-Nanbu earthquake. Observed main damage patterns in the reinforced concrete structures were shear failures of the columns with poor arrangements of the lateral reinforcement. For those columns, confinement of the column sections is effective to improve the ductility of the columns in avoiding the brittle failure. Authors proposed spacing the carbon fiber reinforced polymer (CFRP) strips for the retrofitting of those columns. This paper presents the seismic performance of reinforced concrete columns retrofitted with CFRP strips comparing with those of the columns with CFRP sheet. In this research program, seismic loading tests were performed using scaled reinforced concrete columns in the laboratory of the Hiroshima University. From test results, The columns retrofitted with CFRP strips showed the very good performance as same as CFRP sheet. Moreover, it is anticipated that there is strong possibility of decreasing the amount of CFRP.

1 INTRODUCTION

The seismic evaluations and the developments of the retrofitting techniques for the existing structures against the major earthquakes had been carried out from 1970 in Japan. In 1995 Hyogoken-Nabu earthquake, reinforced concrete columns of building structures were severely damaged resulting considerable loss of life and wealth. Reinforced concrete columns of the rail-way structure were also damaged at that event, resulting inconvenient of the logistics and the rescue. Observed main damage patterns in the reinforced concrete structures were shear failures of the column due to the poor arrangements of the lateral reinforcement. After that event, numerous retrofitting techniques for the existing reinforced concrete structures and strengthening methods for the damaged columns were proposed and then were speedily used in practice. The most effective method for the brittle failure of the columns was the jacketing column sections with the concrete, the steel plates, and the continuous fiber material. Confinement of the column sections improves the ductility of the column against the seismic loadings in avoiding the brittle failure. While the continuous fiber materials had merits of the high strength and the light weight, researches of the fiber reinforced polymer material for the retrofitting to the existing reinforced concrete structures started at the latter half of the 1980 in Japan, Kastumata. In the first international symposium held in Vancouver on March 1993, many techniques using the fiber reinforced polymer materials were reported. In U.S. and Japan, the guidelines of the design using continuous fiber reinforced polymer were published, ACI Committee 440, JSCE 1996, AIJ Committee 2001.

The carbon or glass fiber sheets as retrofitting materials were mainly used in practice to improve the seismic performance of the existing reinforced concrete structures. Though the CFRP sheet is the superior material to confine the column section from the previous studies, it is difficult to inspect visually the damage level of the columns after the earthquake due to the perfectly wrapped sheet. In point of construction view when using sheet it is needed to cut away or cut off the walls from the columns which has the nonstructural walls in the railway station area.

From the disadvantage of the sheet, authors proposed spacing the CFRP strips of tapes and braiding. Besides the immediate inspections or the construction advantage, while spacing the CFRP strips mitigates the concentration of the stress in the CFRP materials it is expected to avoid the fracture of the retrofitting material, leading to the rapid strength degradations of the columns. In this paper the possibility of decreasing the amount of the CFRP is also discussed because the CFRP is expensive.

This paper presents the seismic performance of reinforced concrete columns retrofitted with CFRP strips of tapes and braiding comparing with that of the column retrofitted with CFRP sheet.

In this research program, seismic loading tests were performed using the seven reinforced concrete columns in the laboratory of the Hiroshima University.

2 EXPERIMENTAL PROCEDURE

2.1 *Descriptions of original columns*

The configuration and the details of the seven test columns before retrofitting were common and all test columns were designed as the existing reinforced concrete columns of railway bridges and railway stations. Test columns were designed as the shear failure type according to the old Standard Specifications for Concrete Structures(JSCE) and their ratio of the shear strength V_{yd} to the flexural strength V_{rd} was approximately 0.64.

Seven scaled reinforced concrete columns have been assigned for seismic loadings under the constant axial loads. Test columns had clear height of 1,000mm with a cross section of 300 mm × 300 mm where test columns were 1/3~1/4 scale of prototype rail way columns. Each column had the heavily reinforced stub, which were 1.2m ×1.2m × 0.5m, at the bottom end of the column to fix rigidly at the reaction floor of the laboratory. Figure 1 shows the details of the original test column. The corners of the column sections were round with radios 32 mm to avoid the rupture of the CFRP. Specified strength of concrete Fc was 27N/mm². Concrete were cast from the top of the column as the same condition of the actual construction site using the metal form set. All test columns were reinforced with D19 of longitudinal reinforcing bars and φ6 of transverse reinforcing bars. The total longitudinal reinforcement ratios and the transverse reinforcement ratio were 1.47% and 0.094%, respectively. Table 1, Table 2 and Table 3 show the mechanical properties of the used materials, concrete, steel and CFRP, respectively. Young's Modulus E_f of braiding is less than half of that of tape, but the ultimate strain ε_u of braiding is 1.6 times of that of tape.

Figure 1. Detail of the test columns.

Table 1. Mechanical properties of concrete.

Test Column	Concrete Strength σ_B (N/mm²)	Tensile Strength σ_t (N/mm²)	Young's Modulus E_c (10^4 N/mm²)
JRW05-1	28.36	2.79	3.14
JRW05-2	28.78	2.74	3.14
JRW05-3	29.49	2.76	3.12
JRW05-4	26.19	2.50	3.00
JRW05-5	32.02	2.79	3.26
JRW05-6	27.58	2.97	3.34
JRW05-7	28.54	2.41	2.89

Table 2. Mechanical properties of steel.

Steel bar	Yield Strength σ_y (N/mm²)	Ultimate Strength σ_u (N/mm²)	Young's Modulus E_s (10^5 N/mm²)
Longitudinal steel D19	339	527	1.42
Transverse steel D6	617	713	2.06

Table 3. Mechanical properties of CFRP. (including Epoxy).

CFRP	Strength σ_f (N/mm²)	Young's Modulus E_f (10^5 N/mm²)	Ultimate Strain ε_u (%)
Sheet Tape	3426	2.39	1.46
Braiding	2248	1.06	2.31

2.2 *Retrofitting procedure*

Parameters in the retrofitting procedure for the all test columns are summarized in Table 4. The test columns JRW05-1 was not retrofitted to estimate the effectiveness of the retrofitting with CFRP. The other six test columns were retrofitted with CFRP sheet and strips(tapes and braiding). Test column JWR05-02 was wrapped with the CFRP sheets which consisted of two kinds of the sheet of 300g/m² and 400g/m². Two layers of each sheet were wrapped around the column sections, resulting total amount of the CFRP was 1400g/m². Test columns JRW05-3 and JRW05-4 were retrofitted with CFRP tapes of which width and unit weight were 30mm and 30g/m, respectively. Designed spaces of the tapes were 100mm and 50mm and five layers and three layers of tapes were wrapped for the test columns, resulting the total amounts of the CFRP were 1500g/m² and 1800g/m². Target ductility of the JRW05-2~4 were more than ten. Test columns JWR05-5 and JRW05-6 were prepared with the aim of reducing the amount of the CFRP. One layer of the tapes along the total height of the column was wrapped for JRW05-5 of which the target ductility was five. For JRW05-6, five layers of the tapes were wrapped at the critical area of which length was the column depth D from the bottom end of the column and one layer was wrapped the other area.
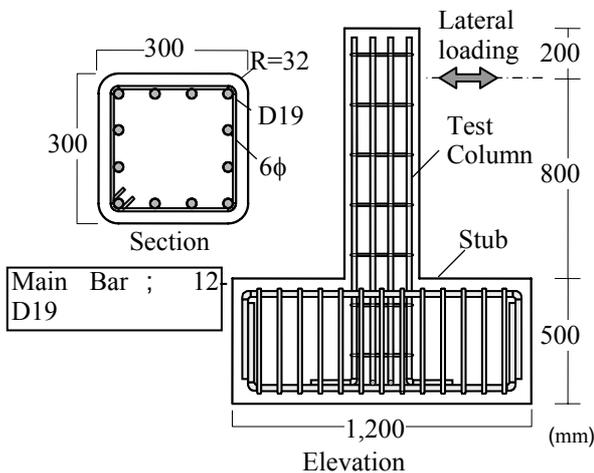
Table 4. List of test columns.

Test Column	CFRP	Width (mm)	Space (mm)	Number of layer	Failure Mode	V_{cyd}/V_{rd}	Target Ductility	Design Ductility from Eq.(1)
JRW05-1	-		-	-	Shear	0.64	-	-
JRW05-2	Sheet		-	4*	Flexural	8.02	10	12.02
JRW05-3	Tape	30	100	5	Flexural	8.54	10	12.62
JRW05-4	Tape	30	50	3	Flexural	10.12	10	14.44
JRW05-5	Tape	30	100	1	Flexural	2.22	5	5.35
JRW05-6	Tape	30	100	5&1**	Flexural	8.54	10	12.62
JRW05-7	Braiding	10	100	5	Flexural	4.97	8	8.52

* Two sheets of 400g/m^2 and 300g/m^2 were layered respectively.

** 5 layers of carbon fiber strips were provided in the area length 1D(column depth) at the bottom end of the column.

Figure 2. CFRP braiding.

For JRW05-7, CFRP braiding shown in Figure 2 was newly proposed in the FRP field. Width of the CFRP braiding was 10mm and its unit weight was the same of the tape.

The amount of CFRP strips were obtained based on the equation (1) proposed for CFRP sheet in Railway Technical Research Institute Guide.

$$\mu = 2.8 + 1.15 \frac{V_{cyd}}{V_{rd}} \qquad (1)$$

μ was the target ductility and V_{cyd} was the shear strength of the column after retrofitting, presenting the sum of the shear strength of the concrete column V_{yd} and the strength of the CFRP V_{cf} as equation (2).

$$V_{cyd} = V_{yd} + V_{cf} \qquad (2)$$

V_{yd} was presented by equation (3) as follows.

$$V_{yd} = V_{cd} + V_{sd} \qquad (3)$$

V_{cd} was the strength of the concrete shear resisting mechanisms, and V_{sd} was the strength of arranged transverse reinforcement. V_{cf} was presented by equation (4) as follows.

$$V_{cf} = \frac{0.8 A_{CF} \cdot f_{CFud}}{S_{CF}} \cdot \frac{Z}{\gamma_{bCF}} \qquad (4)$$

A_{CF}, S_{CF} and f_{CFud} were the sectional area, the width and the tension strength of the unit of CFRP sheet respectively ; $Z=d/1.15$(d was effective depth of the column) ; $\gamma_{bCF}=1.15$.

$$V_{rd} = \frac{M_{cf}}{l_a} \qquad (5)$$

The flexural strength V_{rd} was obtained by dividing

the flexural moment capacity M_{cf}, which was calculated by the fiber model, with shear span l_a=800mm as equation (5). Target ductility and the design ductility of the test columns obtained from the equation (1) using the specified materials are shown in Table 4. The ductility of the test columns JRW05-7 with CFRP braiding was lower than those of the test columns JRW05-3 in spite of using the same amount of CFRP because the strength for the CFRP braiding of 2248N/mm^2 was lower than the strength of the CFRP sheet and tapes of 3426N/mm^2.

2.3 Test setup

The seismic loading tests were conducted in Hiroshima University. The test setup is shown schematically in Figure 3. The stub of the test column was post-tensioned to the reaction floor with the high tension bolts, whose tension force were 300kN per a bolt. The lateral and vertical loading systems displaced the actual column in a canti-lever condition. The shear span ratio was M/QD=2.67. All test columns were subjected to reversal lateral loads under the constant axial load which was 90kN(σ_o=1N/mm^2). Both ends of the vertical and the lateral loading jacks were supported by the pin joints.
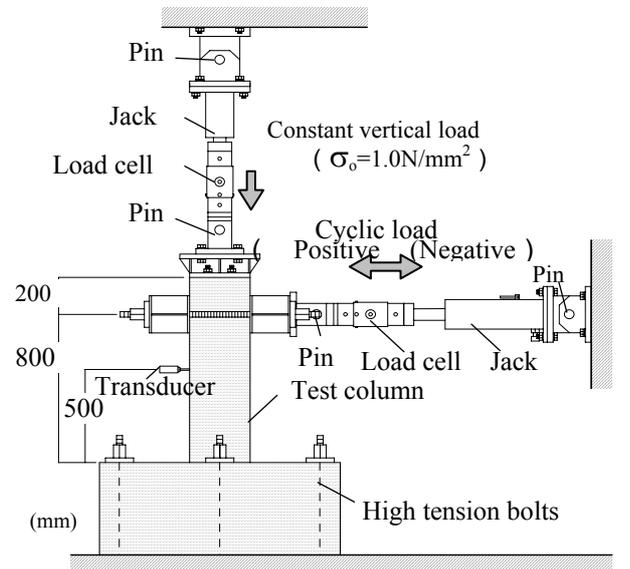

Figure 3. Test setup.

2.4 Measurement system

All test columns were instrumented with number of LVDTs to measure the lateral and the vertical displacement to evaluate the deflection modes and to measure the curvatures of the hinging regions of the columns. The strain gages were mounted on the surfaces of the longitudinal and transverse reinforcing bars to evaluate the yielding and the confinements. Also, the strain gages were mounted on the surface of the CFRP strips at the all side of the rectangular column sections. Both hydraulic jacks for the lateral and the vertical loads were equipped with load cells at the loading points as shown in Figure 3.

2.5 Loading Program

Figure 4 shows the lateral loading program. Before yielding of the longitudinal reinforcing bars lateral loadings were carried out according to the predetermined drift angles, attempting three cycles for the each peak drift angle levels of R=0.00125rad., 0.0025rad., 0.005rad.. Yielding was monitored by the strain of the longitudinal reinforcing bars at the bottom end of the column. After yielding of the longitudinal reinforcing bars the lateral loadings were carried out under ductility level control, attempting three cycle for each of the peak displacement of ductility levels of μ=1,2~10. After ductility ten only one cycle was applied to the test columns at each displacement level up to the limitation of the loading system.
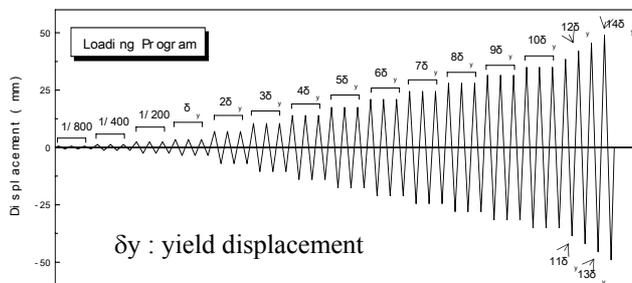

Figure 4. Lateral loading program.

3 TEST RESULTS

3.1 Yield strength and displacement

Table 5 shows the observed yield strength and yield displacements δy of the test columns at the yielding of the longitudinal reinforcing bars. Yield strengths and displacements of the all teat columns were approximately similar except for JWR05-1. For test column JRW05-1 without retrofitting the yielding were not observed while considerable strength degradations occurred due to the shear failure. Yield strains were observed on the way from drift angle 0.005rad. to 0.01rad..

Table 5. Yield strength and displacement.

Test Column	Yield Strength	Yield Displacement*	Drift Angle
	(kN)	(mm)	(10⁻³rad.)
JRW05-1	-	-	-
JRW05-2	190.0	3.23	6.46
JRW05-3	173.5	3.18	6.36
JRW05-4	173.8	3.50	7.00
JRW05-5	185.9	3.49	6.98
JRW05-6	187.8	3.58	7.16
JRW05-7	171.8	3.39	6.78
Ave.	180.5	3.40	6.80

* Displacement measured at the height of the test column 500mm

3.2 Crack pattern and failure modes

The failure patterns for four test columns are illustrated in Figure 5. For JRW05-1 which was not retrofitted diagonal cracks occurred before yielding. The final failure mode was the typical shear failure while scarcely any flexural cracks were observed. For JRW05-2 that was retrofitted with CFRP sheet through the total height of test column, consequently, crack patterns could not be observed visually. Its failure mode was supposed to be flexural type from the lateral displacement distribution while the horizontal cracks widely opened at the bottom end of the test column. At failure stage the sheet at the bottom portion of the test column expanded to out-plane of the column section with spalling and crashing of concrete cover or buckling of the longitudinal reinforcing bars. Failure patterns for other five test columns retrofitted with CFRP strips were approximately similar. Before lateral displacements 6δy shear cracks were observed as same as JRW05-1 and the flexural cracks in parallel with CFRP strips were progressed at the bottom portions of the test columns.
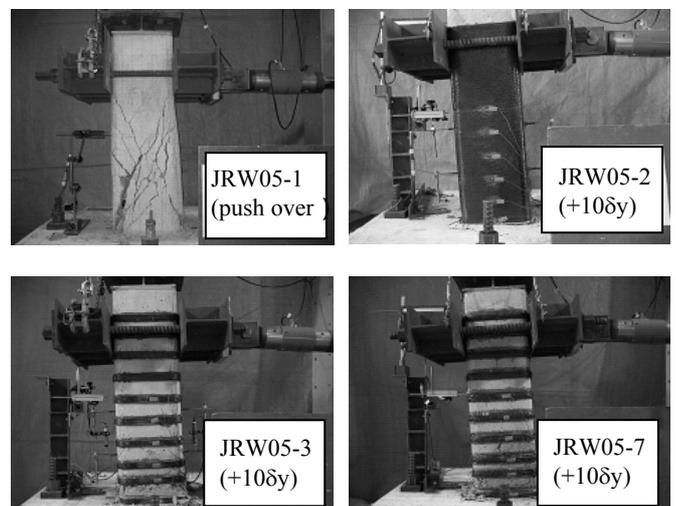

Figure 5. Crack pattern at displacement 10δy.

Width of the shear cracks did not become large due to the confinement of the CFRP strips.

When the displacements became large over 6δy flexural cracks widely opened and crashing of the concrete cover were concentrated at an area that was not confined with the CFRP strips in the lower portions of the test column. The sliding displacement in that area increased among the total lateral displacement of the test column without the large strength degradations in the shear-displacement curves until the final stages.

For JRW05-3, JRW05-4 and JRW05-7 the lengths of the main damaged area were limited in the bottom area of the columns. For JRW05-05 and JRW05-6 the lengths of the area which the diagonal shear cracks extended were two times of the column depth though the width of the shear cracks did not become so large to lead the strength degradations. Through the lateral loadings the fractures of the CFRP strips did not occur except for JRW05-5 that was retrofitted with only one layer of the CFRP tapes. The partial fracture at the joint of the tapes in JRW05-5 was observed when its ductility extremely exceeded the target ductility.

3.3 *Shear force-displacement hysteresis response*

The shear force-displacement hysteresis responses of the four test columns are illustrated in Figure 6. Shear force in the Y-axis were corrected for the lateral force caused by the vertical loads. Lateral displacements at the height of 500 mm in the test columns were used in the X-axis. The white circles in the figures indicated 10δy in the plus and minus direction. Seismic performance of JRW05-1 without retrofitting was very poor due to the shear failure before yielding. Rapid degradation of the lateral shear force was observed after the drift angle 0.005rad. and simultaneously the test column lost the vertical load carrying capacity. Hysteresis responses of the other six test columns retrofitted with CFRP were considerably improved by changing of the failure mechanism from the shear failure to flexural failure. Shear force could be transferred smoothly to the basement due to the confinement effects of the CFRP that protected the progress or the expanding of the shear cracks. In the test columns with retrofitting, the significant strength degradations were not observed at the same displacement reversals. Features of hysteresis responses of four test columns JRW05-2, JRW05-3, JRW05-4 and JRW05-7 were spindle types, which showed flexural behavior, up to the large ductility area. JRW05-04 of which the amount of CFRP was the largest in the test columns had the most stable hysteresis loops. For the other two test columns JRW05-5 and JRW05-6 the pinching phenomena were apparently observed near the origin because the damages due to the shear cracks,
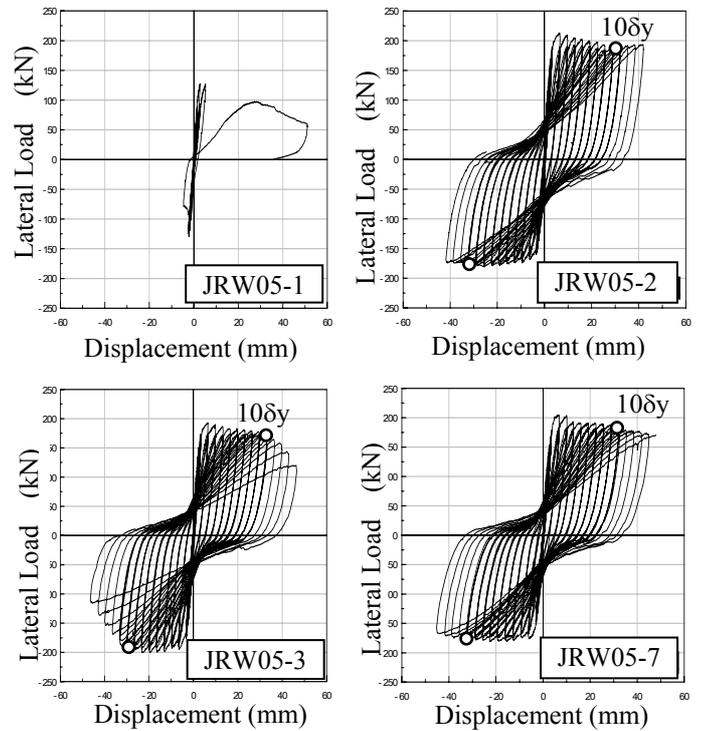

Figure 6. Hysteresis response.

which occurred allover the column height, were relatively severe.

3.4 *Strains in CFRP*

The maximum strain distributions of CFRP strips in the perpendicular directions and in the parallel directions of the lateral loading at each displacement level of JRW05-3 retrofitted with CFRP tapes and JRW05-7 retrofitted with CFPR braiding were illustrated in Figure 7. Strains in the X-axis were represented as the averages of the maximum strains of the CFRP of both sides of the column sections. Displacement levels shown in the figure were of δy, 5δy, 10δy and 14δy. The X-axis of strain was also represented as the ratio to the ultimate strain ε_u of the CFRP.
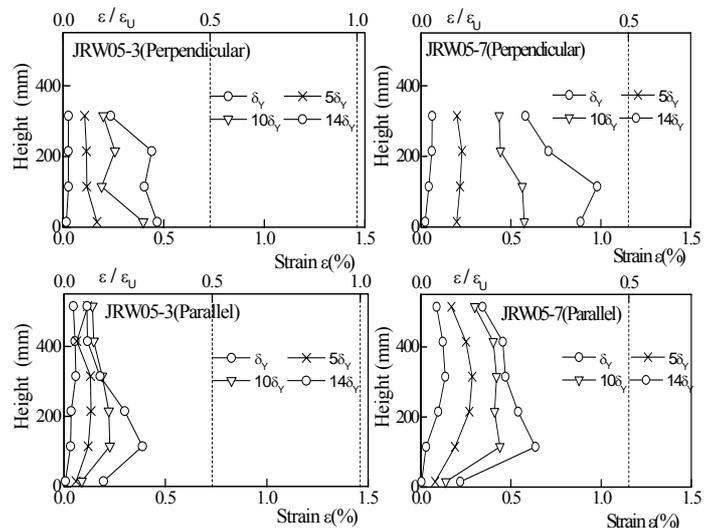

Figure 7. Strain distributions of the CFRP for JRW05-3 and JRW05-7.

Maximum strains gradually increased when the applied displacements increased. For JRW05-3, the maximum strains of the perpendicular direction at $14\delta y$ were approximately less than one third of the ultimate strain ε_u of the CFRP. Maximum strain distributions of the parallel direction at $14 \delta y$ were less than those of the perpendicular direction and were one fourth of the ultimate strain ε_u. Maximum strains of the parallel direction at the bottom end of the columns did not become so large because of the restriction from the rigid stub. The strain distributions of the CFRP braiding for JRW05-7 in the Figure 7 were about two times greater than the strain distributions of the CFRP she tapes. It is indicated that the confined effect of the CFRP braiding was approximately the same of the tape or sheet considering Young's Modulus of the both materials.

In comparison with the strains of the both directions, the strains of the perpendicular direction were greater than the strains of the parallel direction. It is indicated that CFRP strips acted more effectively as confinement of the column section rather than shear protection.

4 DISCUSSIONS

4.1 Envelope curves

Figure 8 shows the envelope curves of the hysteresis loops of the all test columns. There was no difference in the initial stiffness in the all test columns.
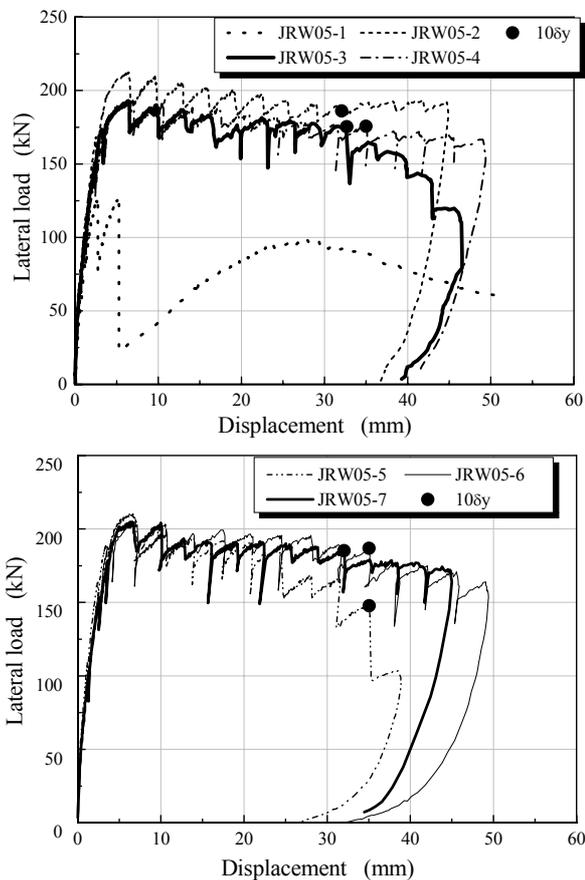

Figure 8. Comparison of the envelope curves.

In the test columns with retrofitting, the peak strength of the applied displacement levels gradually decreased after the maximum strength was recorded. The ductility ten are pointed out in the figure. The strength of JRW05-2 with CFRP sheet was slightly higher than the strength of the other test columns with CFRP strips throughout the lateral loadings. It is indicated that the compressive strength of the concrete and the bond characteristic for the longitudinal reinforcing bars were improved by the CFRP sheet that perfectly confined column sections. In general, large differences between the sheet and the strips were not observed in the envelope curves throughout the lateral loadings. The observed maximum strength and the observed maximum ductility are summarized in Table 6. The maximum ductility was defined as the ductility at the 80% of the maximum strength.

Table 6. Observed maximum ductility.

Test Column	Observed Maximum Strength (kN)	Maximum Strength 80% (kN)	Observed Ductility	Design Ductility
JRW05-1	127.8	102.2	Less than 1	-
JRW05-2	212.8	170.3	Over 14	12.02
JRW05-3	192.9	154.3	12	12.62
JRW05-4	193.7	155.0	Over 14	14.44
JRW05-5	210.3	168.3	8	5.35
JRW05-6	204.1	163.3	Over 14	12.62
JRW05-7	204.8	163.9	Over 14	8.52

Calculated shear strength V_{yd} and calculated flexural strength V_{rd} using the experimentally obtained material strength were 120kN and 174kN, respectively from the equations (3) and (5). The observed maximum strength of JRW05-1 (127.8kN) was approximately the same of the calculated shear strength V_{yd}. The average of the observed strength (203.1kN) of the test columns with retrofitting were 1.17 times of the calculated strength V_{rd} because of the confined effects of the CFRP. Observed maximum ductility of test columns with retrofitting exceeded the target ductility shown in the Table 1. Especially the maximum ductility of JRW05-7 with CFRP braiding was 1.75 times of the target ductility. The strength of JRW05-5 continued to sustain the more than 80% of the maximum strength until ductility reached eight over the target ductility five. After ductility ten, the strength rapidly degreased. It is indicated that the design procedure of the retrofitting with the CFRP sheet is applicable to that for CFRP strips.

4.2 Energy dissipation

Figure 9 shows the relationships between the energy dissipation and the applied maximum displacement of the first cycle at each applied displacement levels. Energy dissipation presented as the equivalent vis-

cous damping factor in this study was one of the most important index to decrease the dynamic responses of the structures during the earthquakes. The equivalent viscous damping factors were obtained by measuring the area of the hysteresis loops.

Initial damping factors of all test columns before yielding were 6~10% that were the general values of the reinforced concrete structures before cracking. When yielding occurred in the test columns the damping factors increased rapidly up to 20% approximately. After yielding damping factor of the JRW05-2 and JRW05-4 continued to increase gradually up to 25%~27%. The damping factors of other test columns with retrofitting were slightly less than those of the former two columns. This difference came from the pinching or the slip phenomena in the hesteresis loops due to the sliding or the shear behavior at the severely damaged area of the columns.
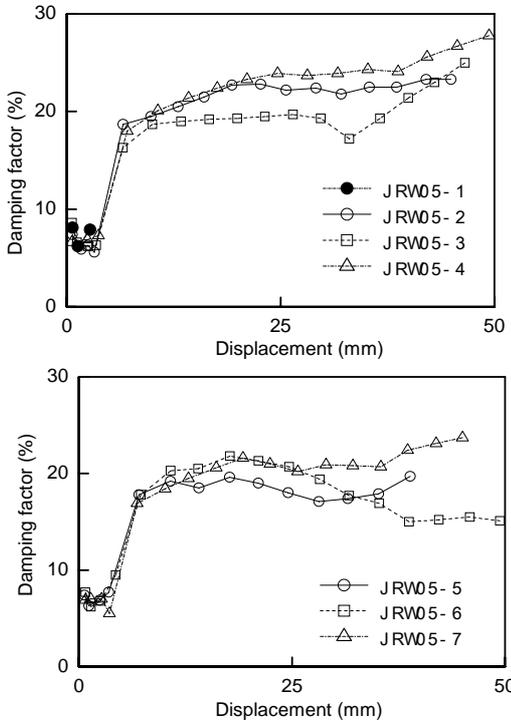

Flexural mode before 6δy   Sliding mode after 6δy

Loading direction

Failure pattern at the final stage of the JRW05-3

Figure 10. Transition of the failure mode.

Figure 9. Progress of energy dissipations.

4.3 Design strength of shear transfer

Before displacement 6δy the displacement distributions of the test columns with retrofitting were the flexural modes while the rotations at the hinging region were predominant in the displacement distributions. After displacement 6δy the displacement distributions of the test columns with CFRP strips except for JRW05-4 changed to the sliding mode when the sliding displacement at one concentrated damaged area became large in the total displacement of the test columns as shown in Figure 10.

It is necessary to evaluate the capacity of the shear transfer by the interlocking of the aggregate and the dowel action of the longitudinal reinforcing bars through the severely damaged area.
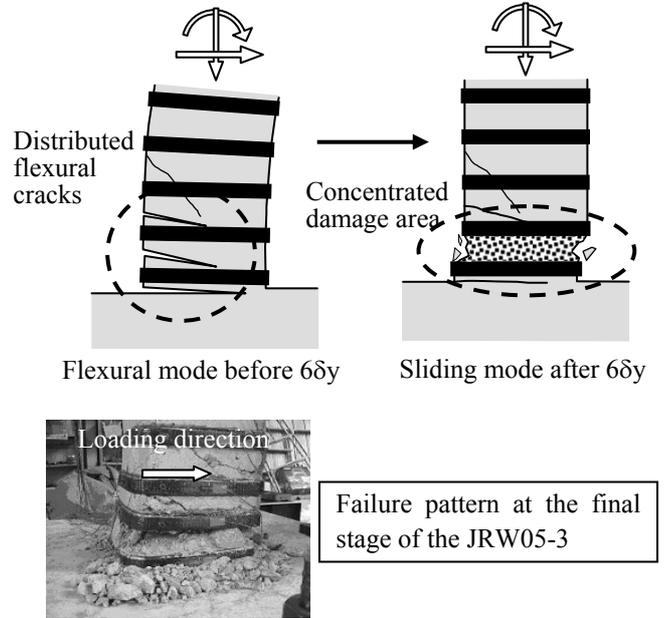
In this section the design strength of the shear transfer obtained by the equations (6) in JSCE Standard was discussed in comparison with the observed maximum strength in the test columns.

$$V_{cwd} = \frac{(\tau_c + p \cdot \tau_s) A_c}{\gamma_b} \quad (6)$$

τ_c and τ_s are the shear transfer stresses of the concrete and the main reinforcing bars, respectively, obtained by the following equations (7) and (8). γ_b is the member coefficient and A_c is the area of the member section.

$$\tau_c = \mu \cdot f_c{}^b (\alpha \cdot p \cdot f_y - \sigma_{nd})^{1-b} \quad (7)$$

$$\tau_s = \frac{0.08 f_y}{\alpha} \quad (8)$$

α in the equation (9) is the reduction factor presenting the degradation of the axial strength for the transverse reinforcing bars and the increase of the shear force. f_c is the concrete strength and f_y is the yield strength of the longitudinal reinforcing bar.

$$\alpha = 0.75 \left\{ 1 - 10 \left(p - 1.7 \frac{\sigma_{nd}}{f_y} \right) \right\} \quad (9)$$

$$0.08 \sqrt{3} \le \alpha \le 0.75$$

In the equation, p is the ratio of the tensile reinforcing bars and σ_{nd} is the average compressive stress perpendicularly acting to the shearing section of the member.

$$\sigma_{nd} = -\frac{1}{2} \frac{(P_{sc} + P_{cc})}{A_{cc}} \quad (10)$$

P_{sc} and P_{cc} are the compressive forces at the compressive reinforcing bars and the concrete of the section, respectively. A_{cc} is the compressive area of the member section.

$$b = \frac{2}{3}, \quad \mu = 0.45, \quad \gamma_b = 1.3$$

μ is the average coefficient of friction, b is the coefficient for the cracked section of the member.

The location of the neutral axis of the column section at the yielding of the longitudinal reinforcing bars was calculated from the equilibrium of the axial force of the column section using the design strength of the materials as shown in Figure 11. It is assumed that the Young's Modulus of the steel and the concrete are 2.0×10^5 N/mm^2 and 2.5×10^4 N/mm^2, respectively, and both materials remain in elastic.

f_{sy}=295N/mm^2
f_c=27N/mm^2
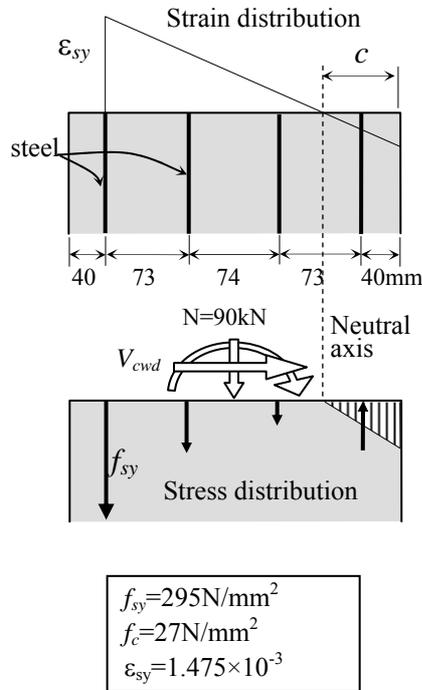ε_{sy}=1.475$\times10^{-3}$

Figure 11. Stress distribution of the member section.

The calculated results are summarized in Table 7. Calculated neutral axis located in the assumed area that was 40mm$<c<$113mm. Calculated design strength of the shear transfer V_{cwd} (=683.3kN) is over three times of the observed maximum strength which were approximately 200kN. It is noted that shear force subjected to the columns can be transferred sufficiently through the severely damaged area of the test column to the basement. On the other hand, the average friction coefficient that was assumed to be 0.45 in this case might be evaluated as larger value than the actual value because the concrete of the sliding zone were severely damaged due to the numerous cyclic loadings.

Table 7. Design strength of shear transfer.

c	P_{sc}	P_{cc}	p
104.4mm	140.2kN	387.4kN	0.0147
α	τ_c	τ_s	V_{cwd}
0.276	8.613	85.51	683.3kN

5 CONCLUSIONS

Seismic loading tests of the scaled reinforced columns retrofitted with the CFRP sheet and strips were performed. The following conclusions were made.
1) Seismic performance of the reinforced concrete columns retrofitted with spaced CFRP strips showed the same performance of the column with CFRP sheet providing the same amount of CFRP. It is indicated that the equations of the evaluation for the CFRP sheet is applicable to that for spaced CFRP strips.
2) When using spaced CFRP strips the damage level of the column could be easily estimated with visual inspection after earthquake.
3) Fracture of the CFRP was avoidable while the damages of the column were concentrated to the bare concrete section between spaced CFRP strips.
4) The displacement distributions changed from the flexural mode to the sliding mode at the concentrated damaged area at the lower portion of the test column retrofitted with spaced CFRP strips.
5) Calculated design strength of the shear transfer is over three times of the observed maximum strength. The shear force could be sufficiently transferred through the severely damaged area.
6) It is anticipated that there is strong possibility of decreasing the amount of the CFRP.

REFERENCES

ACI Committee 440, "State-of-the Art Report on fiber Reinforced Plastics Reinforcement for Concrete Structure (ACI440R-96)"American Concrete Institute, 1996
AIJ Committee "Design and Construction Guideline of Continuous Fiber Reinforced Concrete" Architectural Institute of Japan, 2001
JSCE "Design and Construction Guideline of Continuous Fiber Reinforced Structure" Japan Society of Civil Engineering, 1996
JSCE "Standard Specifications for Concrete Structures", 2002
Katsumata, H., Kobatake, Y., and Takeda, T. "A Study on Strengthening with Carbon Fiber for Earthquake-Resistant Capacity of Existing Reinforced Concrete Columns "*Proceedings of the 9th conference on Earthquake Engineering*, Vol.7, Tokyo, Japan, Aug. 1988, pp.517-522
Railway Technical Research Institute : Guide for retrofitting design for the railway column with carbon fiber sheet, JCAA, Tokyo